

## Climatic influences on the offset between $\delta^{18}\text{O}$ of cave drip waters and precipitation inferred from global monitoring data

Andy Baker<sup>1</sup>, Wuhui Duan<sup>1,2</sup>, Mark Cuthbert<sup>3,1</sup>, Pauline Treble<sup>4,1</sup>, Jay Banner<sup>5</sup>, Stuart Hankin<sup>4</sup>

<sup>1</sup>Connected Waters Initiative Research Centre, UNSW Sydney, Sydney 2052, Australia

<sup>2</sup>Key Laboratory of Cenozoic Geology and Environment, Institute of Geology and Geophysics, Chinese Academy of Sciences, Beijing, China, 100029

<sup>3</sup>School of Earth and Ocean Sciences, Cardiff University, Cardiff, UK

<sup>4</sup>Australian Nuclear Science and Technology Organisation, Lucas Heights 2234, Australia

<sup>5</sup>Jackson School of Geosciences, The University of Texas at Austin, 2305 Speedway, Austin TX 78712, USA.

**Abstract:** We present a meta-analysis of data from 22 caves and 96 drip sites from 4 continents where both the cave drip water  $\delta^{18}\text{O}$  and the weighted mean  $\delta^{18}\text{O}$  of precipitation have been measured. Drip water  $\delta^{18}\text{O}$  is similar to the weighted mean  $\delta^{18}\text{O}$  of precipitation (within  $\pm 0.3$  ‰) for sites where mean annual temperature (MAT) is less than 15 °C (85% of drips where MAT < 15 °C) and an aridity index (annual precipitation (P) / annual potential evapotranspiration (PET)) is greater than 0.65 (74% of drips at sites where P/PET > 0.65). In contrast, at warmer locations with increased water deficit, drip water  $\delta^{18}\text{O}$  deviates from the weighed mean precipitation  $\delta^{18}\text{O}$  by +3 ‰ and -1.5 ‰. We argue that this is due to evaporation in the soil and shallow vadose zone (thereby increasing drip water  $\delta^{18}\text{O}$ ) and lower water storage in the vadose zone, leading to relatively less mixing (thereby increasing the range in drip water  $\delta^{18}\text{O}$  to more closely reflect recharge water  $\delta^{18}\text{O}$ ). Speleothems that have formed close to isotopic equilibrium are likely to have an oxygen isotope composition that contains a mixed signal of cave air temperature and precipitation  $\delta^{18}\text{O}$  only in cool and temperate regions (T < 15 °C), or very wet climates where P/PET >> 0.65. In contrast, in warmer and drier environments, speleothems which have formed close to equilibrium will have  $\delta^{18}\text{O}$  that reflects cave air temperature and a seasonal bias toward the  $\delta^{18}\text{O}$  composition of rain in periods of high recharge, as well as the extent of evaporative fractionation of stored karst water.

### Introduction

Speleothem  $\delta^{18}\text{O}$  is the most widely reported climate proxy in cave stalagmites, stalactites and flowstones (Hartman and Baker, 2017). Speleothem  $\delta^{18}\text{O}$  is determined by multiple processes: the potential climate signal being the source water  $\delta^{18}\text{O}$  composition and its relationship to local and regional climate. This signal is transferred to the cave through the vadose zone, where it may be mixed with existing waters and fractionated by evaporation. Finally, at the target, the speleothem, the  $\delta^{18}\text{O}$  signal can be further altered by non-equilibrium fractionation processes and a temperature dependent fractionation during calcite precipitation. Reviews of these processes and signal transformation include Lachinet (2009), Fairchild and Baker (2012), and Hartmann and Baker (2017).

Within the speleothem research community, it has been recognised that to understand the  $\delta^{18}\text{O}$  climate signal transfer from source to target, a cave monitoring approach would be beneficial. The measurement of drip water hydrology (Smart and Friedrich, 1986), drip water geochemistry (Pitty, 1966), cave climatology (Wigley, 1977), and calcite growth and geochemistry (Mickler et al., 2006) as well as surface climate parameters, allows empirical relationships between cave parameters and climate to be determined. Monitoring data could be used to determine regression models between climate and speleothem proxy (for example, Baker et al., 2015), evaluate proxy interpretation (Feng

et al., 2014), provide input data for forward, or proxy system models (Evans et al., 2013; Deininger et al., 2014; Bradley et al., 2010; Truebe et al., 2010), and assess the extent to which speleothem calcite forms in isotopic equilibrium with its associated drip water (Mickler et al., 2004, 2006; Feng et al., 2012).

A considerable number of speleothem  $\delta^{18}\text{O}$  records have been published and archived: for example 300+ records within the last 21ka have been identified by SISAL (Comas Bru et al., 2018). Some regions have speleothem  $\delta^{18}\text{O}$  records that provide records of glacial-interglacial climate change (e.g. monsoon regions; Wang et al., 2001; Cheng et al., 2016; Wang et al., 2017). However, other regions have speleothem  $\delta^{18}\text{O}$  records that are more complex. For example, water-limited regions where  $\delta^{18}\text{O}$  has high magnitude and frequency variability (e.g. Dennison et al., 2013; Treble et al., 2017). In water-limited environments, several potential mechanisms have been proposed to significantly affect speleothem  $\delta^{18}\text{O}$ , including: 1) evaporative fractionation of  $\delta^{18}\text{O}$  in the soil, shallow vadose zone or cave; 2) selective recharge, whereby rainfall events with high magnitude or intensity have a distinct isotopic composition, typically low  $\delta^{18}\text{O}$ ; and 3) non-equilibrium deposition during speleothem formation (Cuthbert et al., 2014; Pape et al., 2010; Dreybrodt and Scholz, 2011; Markowska et al., 2016). A fundamental research question is: what are the climate parameters where speleothem  $\delta^{18}\text{O}$  may most likely record the source signal, the  $\delta^{18}\text{O}$  of precipitation? Such climatic regions, and speleothem samples, will have the greatest utility for research methodologies which utilise proxy – climate model inter-comparison (e.g. data assimilation, Goose 2016).

Interpretation of speleothem  $\delta^{18}\text{O}$  archives would benefit from the best possible understanding of the climatic conditions under which drip water  $\delta^{18}\text{O}$  is most directly related to precipitation  $\delta^{18}\text{O}$ . Here, we compile cave monitoring data, with the objective of understanding the modern-day relationship between precipitation  $\delta^{18}\text{O}$  and drip water  $\delta^{18}\text{O}$ . We compile datasets where there are both cave drip water data and surface precipitation  $\delta^{18}\text{O}$  data. Results are compared to climate parameters, and implications for speleothem oxygen isotope paleoclimatology are discussed.

## Methods

Drip water  $\delta^{18}\text{O}$  data were compiled from a literature search. To minimise uncertainties that could be introduced into our analysis, we have chosen to only include sites where both of the following two criteria were met: (1) precipitation  $\delta^{18}\text{O}$  was collected at or close to the sites, for at least one year, with an amount weighted mean value reported. (2) drip water  $\delta^{18}\text{O}$  was collected over the hydrological year, for at least one year. Monitoring results had to have at least 1-year of both drip water and precipitation  $\delta^{18}\text{O}$  data, with overlapping time periods. We therefore have not included sites where  $\delta^{18}\text{O}_p$  is a derived parameter e.g. from isotope enabled GCM output or based on empirical relationship with distant Global Network of Isotopes in Precipitation (GNIP) stations.

Drip water and weighted mean of precipitation data were compared to the following climate characteristics: mean annual temperature (MAT), total annual precipitation (P), potential evapotranspiration (PET) and an aridity index (P/PET). PET and the aridity index were taken from the global aridity and PET database (Zomer et al, 2007; 2008), where PET is modelled at approximately 1 km resolution using data from the WorldClim Global Climate Database using mean monthly extra-terrestrial radiation, and mean monthly temperature mean and range (using the equation of Hargreaves, 1985). The aridity index is classified as humid at an aridity index  $> 0.65$ ; semi-arid and dry

sub-humid sites are 0.2 to 0.65, and arid and hyper-arid sites <0.2. The difference between the weighted mean of precipitation and drip water  $\delta^{18}\text{O}$  was determined for each drip site ( $\Delta_{p-dw}$ ).

## Results and Discussion

Table 1 presents the database compiled from the meta-analysis, with data drawn from ten publications. It comprises 96 drip sites from 22 caves on 4 continents: Australia (Goede et al., 1983; Cuthbert et al., 2014; Treble et al., 2015; Tadros et al., 2017); Asia (Duan et al., 2016; Moerman et al., 2013); Europe (Fuller et al., 2008; Genty et al., 2014) and North America (Pape et al., 2010; Feng et al., 2014). For each site, the local MAT and total annual P were taken from the publications, and PET taken from the WorldClim Global Climate Database. For one study (Moerman et al., 2013), total annual precipitation was not provided and output from the gridded dataset was used instead. The aridity index was calculated from the local P and gridded PET. The location of the caves in comparison with two of the climate parameters (MAT and the aridity index P/PET) are shown in Figure 1.

As cross-checks on the gridded database, we compared for all caves local P and gridded P (Eqn. 1) and local T and gridded T (Eqn. 2), and for the Australian caves we compared gridded PET with the mean PET (1960-1990 AD) calculated from the Australian Water Availability Project (AWAP) and AWRA-L databases (Raupach et al., 2009, 2011; Viney et al., 2015):

$$\text{Gridded P} = 1.04 \text{ P} \quad (r = 0.98) \quad (1)$$

$$\text{Gridded T} = 0.996 \text{ T} \quad (r = 0.96) \quad (2)$$

For the Australian sites, the gridded PET calculated by the two products agreed within 7% for all sites except Golgotha Cave, where the AWRA-L PET was 30% higher than that calculated by Worldclim. The difference in PET at this site did not change the aridity index classification (using Worldclim: 1.06; using AWRA-L 0.82), and the Worldclim data is used for consistency.

Climate regimes represented in the compilation include temperate maritime and semi-arid, monsoon, mediterranean, montane, and tropical. Poorly represented are tropical climates (just two caves, from Moerman et al., 2013) and unrepresented are cold climates (no caves with MAT < 6 °C).

Figure 2 presents correlation matrices for the climate parameters (MAT, total annual P, PET, aridity index), the weighted mean  $\delta^{18}\text{O}$  of precipitation, the mean  $\delta^{18}\text{O}$  of drip water, and  $\Delta_{p-dw}$ , the difference between water and weighted mean precipitation  $\delta^{18}\text{O}$  composition. Also presented are histograms of each parameter as their frequency distribution. At this global scale, we see positive correlations between annual MAT and PET ( $R^2 = 82\%$ ) and total annual P and P/PET ( $R^2 = 77\%$ ), and a weak negative correlation between PET and P/PET ( $R^2 = 52\%$ ). The correlations between  $\delta^{18}\text{O}$  of drip water and weighted mean precipitation  $\delta^{18}\text{O}$  is positive and strong ( $R^2=83\%$ ), indicating that at a global scale,  $\delta^{18}\text{O}$  of drip water can be explained by the  $\delta^{18}\text{O}$  of precipitation (equation 3).

$$\delta^{18}\text{O}_{dw} = 0.73 (\pm 0.32) + 1.07 (\pm 0.05) \delta^{18}\text{O}_p \quad (\text{per mille}) \quad (3)$$

Equation 1 also demonstrates an empirical relationship from our dataset of 96 drip sites from 22 caves, that drip water  $\delta^{18}\text{O}$  is more positive than the weighted mean of precipitation.

Figure 3 explores the relationship between  $\delta^{18}\text{O}$  of the weighted mean of precipitation and  $\delta^{18}\text{O}$  drip water in more detail. For all 96 drip sites, the relationship between  $\Delta_{p-dw}$  and each of the climate parameters are presented in scatter plots. It can be observed that there is a narrowing in the range of  $\Delta_{p-dw}$  when MAT is relatively low ( $< 15\text{ }^\circ\text{C}$ ). The range of  $\Delta_{p-dw}$  also decreases for sites with high total annual P ( $> 1900\text{ mm}$ ) low annual PET ( $< 800\text{ mm}$ ) and high total aridity index values ( $> 0.65$ ).

To quantify the relationship between  $\Delta_{p-dw}$  and the climate parameters, we defined an arbitrary threshold for 'acceptable'  $\Delta_{p-dw}$  of less than  $0.3\text{ }‰$ . This was chosen taking in to consideration potential uncertainties in  $\delta^{18}\text{O}$  determinations of water and speleothem calcite (analytical uncertainties of  $0.06\text{--}0.2\text{ }‰$ , depending on measurement technique). Considering the climate parameter MAT, 85 % of sites with a MAT  $< 15\text{ }^\circ\text{C}$  has a  $\Delta_{p-dw}$  of  $< 0.3\text{ }‰$ . Considering the aridity index, as this subsumes P and PET, then for a P/PET threshold of 0.65, the definition of 'humid', 74% of all sites with P/PET  $> 0.65$  have a  $\Delta_{p-dw}$  of  $< 0.3\text{ }‰$ . With data from only three caves where total annual P  $> 1900\text{ mm}$ , further data from sites with high P would be beneficial.

At sites where MAT  $> 15\text{ }^\circ\text{C}$ , the absolute value of  $\Delta_{p-dw}$  ( $|\Delta_{p-dw}|$ ) is greater than the threshold of  $0.3\text{ }‰$  for 84% of the drips. When P/PET  $< 0.65$ ,  $|\Delta_{p-dw}|$  is greater than the threshold at 69% of the drips. The drip water  $\delta^{18}\text{O}$  at these sites have been interpreted by the authors as reflecting either evaporative fractionation of the water in the soil or shallow karst ( $\Delta_{p-dw} < 0.3\text{ }‰$ ) (Cuthbert et al., 2014, Duan et al., 2016) or a bias to recharge from isotopically light rainfall events due to selective recharge ( $\Delta_{p-dw} > 0.3\text{ }‰$ ) (Pape et al., 2010; Feng et al., 2014).  $|\Delta_{p-dw}|$  is less than  $0.3\text{ }‰$  at 16% of drips where MAT  $> 15\text{ }^\circ\text{C}$  and 31 % of drips where P/PET  $< 0.65$ . Post-infiltration evaporative fractionation of isotopically light recharge could lead to these observations.

For  $|\Delta_{p-dw}|$  likely to be less than  $0.3\text{ }‰$ , our meta-analysis shows that a MAT  $< 15\text{ }^\circ\text{C}$ , or high P/PET  $> 0.65$  are required. These climate parameters decrease the opportunity for soil and shallow karst evaporation and can help maintain well-mixed karst water stores that buffer the isotopic impact of any individual recharge event. Speleothems that have been deposited close to equilibrium would have the potential of recording past records of rainfall  $\delta^{18}\text{O}$  composition, plus a temperature signal from the fractionation during calcite precipitation. The locations of the caves sites in comparison to the MAT  $< 15\text{ }^\circ\text{C}$  and P/PET  $> 0.65$  thresholds is shown in Figure 4.

Using our thresholds for  $|\Delta_{p-dw}|$  likely to be less than  $0.3\text{ }‰$ , latitudes poleward of  $\sim 35\text{ }^\circ$  would be most likely to contain this signal (MAT  $< 15\text{ }^\circ\text{C}$ ; northern Europe, northern regions of the Asian monsoon, northern North America, New Zealand), as well as sites with high P/PET (maritime and monsoonal climates; low latitude sites under the ITCZ). In contrast, speleothem  $\delta^{18}\text{O}$  records in regions of higher T and lower P/PET are more likely to have  $|\Delta_{p-dw}| > 0.3\text{ }‰$  and would be sensitive to moisture balance changes due to limited mixing with stored water, and/or increased chance of evaporative fractionation of  $\delta^{18}\text{O}$ . Drip water  $\delta^{18}\text{O}$  can be more positive than precipitation (evaporation dominates) or less than precipitation (selective recharge dominates). Using our thresholds of MAT  $> 15\text{ }^\circ\text{C}$  or P/PET  $< 0.65$ , regions where this mixed signal dominates are predominantly between latitudes  $10$  and  $40\text{ }^\circ$  (most of Africa, India, southern Asia, southern Europe and North America, and Australia). In addition, when considering speleothem  $\delta^{18}\text{O}$ , any relationship between drip water and the  $\delta^{18}\text{O}$  of precipitation could be additionally overprinted by non-equilibrium deposition.

## Conclusions

A meta-analysis of cave drip water and precipitation monitoring records identifies sites and regions where  $\Delta_{p-dw}$  is likely to be closest to zero. These regions could produce speleothem  $\delta^{18}O$  archives, if the speleothems are deposited close to equilibrium, where speleothem  $\delta^{18}O$  could be used in proxy – model assimilation and to provide a mixed signal of past precipitation  $\delta^{18}O$  and cave air temperature. These sites are more likely to be characterised by lower temperatures and more positive water balance. In such systems, karst stores and fractures more likely to be well mixed, one would also expect greater agreement in  $\delta^{18}O$  between drip sites within a cave. In regions with higher temperatures and lower water balance, speleothem  $\delta^{18}O$  is less likely to represent weighted mean  $\delta^{18}O$  of precipitation, and instead can contain a mixed signal that includes selective recharge and evaporative fractionation. Such records are of paleoclimatic value but are more likely to show greater heterogeneity between coeval records and therefore require a drip-specific interpretation.

Important Quaternary speleothem  $\delta^{18}O$  records have been produced from around the world, and in the context of this meta-analysis of modern conditions we can make several conclusions. Firstly, many paleoclimate studies make great use of interpreting relative changes in speleothem  $\delta^{18}O$  over time, and in many cases monitoring data is not available to guide the interpretation. The climatic controls made here can be used to help guide the interpretation of those records. This is particularly relevant over periods of significant climate change (e.g. glacial – inter-glacial transitions) and where the climate control on the rainfall – drip water  $\delta^{18}O$  relationship may change over time. Secondly, in the Chinese monsoon region, the cooler northern sites are most likely to have drip water  $\delta^{18}O$  similar to  $\delta^{18}O_p$ , as reported by Duan et al., (2016). Given that monsoon rainfall requires a land-ocean T gradient, there is trade-off between caves at cooler locations that have drip water  $\delta^{18}O$  closest to precipitation  $\delta^{18}O$ , and those in regions with the strongest monsoon signal. The latter are more likely to experience evaporative fractionation and selective recharge, and therefore less likely to be similar to precipitation  $\delta^{18}O$ . This trade-off would apply to all monsoon regions. Working in caves at altitude within such regions would be advantageous e.g. Sanbao Cave, at 1900m elevation, has a MAT of 8 °C and annual P of 1950 mm (Cheng et al., 2016), and could be expected to have drip water  $\delta^{18}O$  similar to  $\delta^{18}O_p$ . Thirdly, even in regions of exceptionally high rainfall, such as Mulu and parts of India, drip water  $\delta^{18}O$  can be higher than the weighted mean precipitation  $\delta^{18}O$  (Moerman et al., 2013), probably due to the continuous high temperatures leading to the partial evaporation of vadose water. Again, analysis of speleothems at caves at higher elevations should help mitigate this effect. Finally, speleothem  $\delta^{18}O$  records from regions with increasing aridity and higher temperatures should be expected to not preserve a record of precipitation  $\delta^{18}O$ . Our meta-analysis confirms the modern monitoring observations of Markowska et al. (2016), who proposed that speleothem  $\delta^{18}O$  would be an archive of alternating paleo-aridity and paleo-recharge, and supports the interpretation of speleothem  $\delta^{18}O$  as a paleo-recharge and paleo-aridity for the Last Glacial Maximum speleothem in arid southern Australia (Treble et al., 2017).

## References

Baker, A., Hellstrom, J.C., Kelly, B.F.J., Mariethoz, G. and Trouet, V. 2015 A composite annual-resolution stalagmite record of North Atlantic climate over the last three millennia. *Scientific Reports*, 5:10307

- Bradley, C., Baker, A., Jex, C.N., Leng, M.J., 2010. Hydrological uncertainties in the modelling of cave drip-water  $\delta^{18}\text{O}$  and the implications for stalagmite palaeoclimate reconstructions. *Quat. Sci. Rev.* 29, 2201–2214
- Cheng, H., Edwards, R.L., Sinha, A., Spötl, C., Yi, L., Chen, S., Kelly, M., Kathayat, G., Wang, X., Li, X., Kong, X., Wang, Y., Ning, Y., Zhang, H., 2016. The Asian monsoon over the past 640,000 years and ice age terminations. *Nature* 534, 640–646
- Cuthbert, M.O., Baker, A., Jex, C.N., Graham, P.W., Treble, P., Andersen, M.S and Acworth, R.I., 2014 Drip water isotopes in semi-arid karst: implications for speleothem paleoclimatology. *Earth and Planetary Science Letters*, 395, 194-204
- Deininger, M., Fohlmeister, J., Scholz, D., Mangini, A., 2012. Isotope disequilibrium effects: The influence of evaporation and ventilation effects on the carbon and oxygen isotope composition of speleothems - A model approach. *Geochim. Cosmochim. Acta* 96, 57–79
- Denniston, R.F., Wyrwoll, K.H., Asmerom, Y., Polyak, V.J., Humphreys, W.F., Cugley, J., Woods, D., LaPointe, Z., Peota, J. and Greaves, E. (2013) North Atlantic forcing of millennial-scale Indo-Australian monsoon dynamics during the Last Glacial period. *Quaternary Science Reviews* 72, 159-168. Dreybrodt, W., Scholz, D., 2011. Climatic dependence of stable carbon and oxygen isotope signals recorded in speleothems: From soil water to speleothem calcite. *Geochim. Cosmochim. Acta* 75, 734–752
- Duan, W., Ruan, J., Luo, W., Li, T., Tian, L., Zeng, G., Zhang, D., Bai, Y., Li, J., Tao, T., Zhang, P., Baker, A. and Tan, M. 2016. The transfer of seasonal isotopic variability between precipitation and drip water at eight caves in the monsoon regions of China. *Geochimica et Cosmochimica Acta*, 183, 250-266
- Evans, M.N., Tolwinski-Ward, S.E., Thompson, D.M., Anchukaitis, K.J., 2013. Applications of proxy system modeling in high resolution paleoclimatology. *Quat. Sci. Rev.* 76, 16–28.
- Fairchild, I.J., Baker, A., 2012. Speleothem science: from process to past environments. John Wiley & Sons.
- Feng, W., Banner, J. L., Guilfoyle, A., Musgrove, M., and James, E. W., 2012, Oxygen isotopic fractionation between drip water and speleothem calcite: A 10-year monitoring study, central Texas, USA. *Chemical Geology*, 304-305, 53-67
- Feng, W., Casteel, R.C., Banner, J.L. and Heinze-Fry, A., 2014. Oxygen isotope variations in rainfall, drip-water and speleothem calcite from a well-ventilated cave in Texas, USA: assessing a new speleothem temperature proxy. *Geochimica et Cosmochimica Acta*, 127, 233-250.
- Fuller, L., Baker, A., Fairchild, I.J., Spötl, C., Marca-Bell, A., Rowe, P. and Dennis, P.F., 2008. Isotope hydrology of dripwaters in a Scottish cave and implications for stalagmite palaeoclimate research. *Hydrology and Earth System Sciences*, 12, 1065-1074
- Genty, D., Labuhn, I., Hoffmann, G., Danis, P.A., Mestre, O., Bourges, F., Wainer, K., Massault, M., Van Exter, S., Régnier, E., Orengo, P., Falourd, S., Minster, B., 2014. Rainfall and cave water isotopic relationships in two South-France sites. *Geochim. Cosmochim. Acta* 131, 323–343

- Goede, A., Green, D.C and Harmon, R.S., 1983. Isotopic composition of precipitation, cave drips and actively forming speleothems at three Tasmanian cave sites. *Helveta*, 20, 116-126.
- Goose, H., 2016. Reconstructed and simulated temperature asymmetry between continents in both hemispheres over the last centuries. *Climate Dynamics*,
- Hargreaves, G.L., Hargreaves, G.H., Riley, J.P., 1985. Irrigation water requirements for Senegal River Basin. *J. Irrig. Drain. Eng. ASCE* 111 (3), 265-275.
- Hartmann, A. and Baker, A. 2017. Modelling karst vadose zone hydrology and its relevance for paleoclimate reconstruction. *Earth Science Reviews*, 172, 178-192
- Lachinet, M.S., 2009. Climatic and environmental controls on speleothem oxygen-isotope values. *Quaternary Science Reviews*, 28, 314-432.
- Markowska, M., Baker, A., Andersen, M.S., Jex, C.N., Cuthbert, M.O., Rau, G.C., Graham, P.W., Rutledge, H., Mariethoz G., Marjo, C.E., Treble, P.C. and Edwards, N., 2016. Semi-arid zone caves: Evaporation and hydrological controls on  $\delta^{18}\text{O}$  drip water composition and implications for speleothem paleoclimate reconstructions. *Quaternary Science Reviews*, 131, 285-301.
- Mickler, P.J., Banner, J.L., Stern, L., et al. 2004 Stable isotope variations in modern tropical speleothems: evaluating equilibrium vs. kinetic effects. *Geochimica et Cosmochimica Acta*, 68, 4381-4393.
- Mickler, P.J., Stern, L. & Banner, J.L. 2006 Large kinetic isotope effects in modern speleothems. *Geological Society of America Bulletin*, 118, 65-81.
- Moerman, J.W., Cobb, K.M., Adkins, J.F., Sodemann, H., Clark, B. and Tuen, A.A., 2013. Diurnal to interannual rainfall  $\delta^{18}\text{O}$  variations in northern Borneo driven by regional hydrology. *Earth and Planetary Science Letters*, 369-370, 108-119
- Pape, J.R., Banner, J.L., Mack, L.E., Musgrove, M. and Guilfoyle, A., 2010. Controls on oxygen isotope variability in precipitation and cave drip waters, central Texas, USA. *Journal of Hydrology*, 385, 203-215.
- Partin, J.W., Cobb, K.M., Adkins, J.F., Tuen, A.A. and Clark, B., 2013. Trace metal and carbon isotopic variations in dripwater and stalagmite geochemistry from northern Borneo. *Geochemistry, geophysics, geosystems*, 14, 3567-3585.
- Smart, P.L., Friederich, H., 1987. Water movement and storage in the unsaturated zone of a maturely karstified carbonate aquifer, Mendip Hills, England, in: *Proceedings of the Environmental Problems in Karst Terranes and Their Solutions Conference*. National Water Well Association, Dublin OH, pp. 56–87
- Tadros, C. V., Treble, P. C., Baker, A., Fairchild, I., Hankin, S., Roach, R. Markowska, M. and McDonald, J., 2016. ENSO - cave drip water hydrochemical relationship: A 7-year dataset from south-eastern Australia. *Hydrology and Earth System Sciences*, 20, 4625-4640

Treble, P.C., Fairchild, I.J., Griffiths, A., Baker, A., Meredith, K.T., Wood, A. and McGuire, E., 2015. Impacts of cave air ventilation and in-cave prior calcite precipitation on Golgotha Cave dripwater chemistry, southwest Australia. *Quaternary Science Reviews*, 127, 61-72

Treble, P. C., Baker, A., Ayliffe, L. K., Cohen, T. C., Hellstrom, J. C., Gagan, M. K., Frisia, S., Drysdale, R. N., Griffiths, A. D., and Borsato, A., 2017. Hydroclimate of the Last Glacial Maximum and deglaciation in southern Australia's arid margin interpreted from speleothem records (23–15 ka), *Clim. Past* 13, 667-687.

Truebe, S.A., Ault, T.R., Cole, J.E., 2010. A forward model of cave dripwater  $\delta^{18}\text{O}$  and application to speleothem records. *IOP Conf. Ser. Earth Environ. Sci.* 9, 12022.

Viney, N., Vaze J., Crosbie R., Wang B., Dawes W. and Frost A (2015) AWRA-L v5.0: technical description of model algorithms and inputs. CSIRO, Australia.

Wang, X., Edwards, R.L., Auler, A.S., Cheng, H., Kong, X., Wang, Y., Cruz, F.W., Dorale, J.A., Chiang, H.-W., 2017. Hydroclimate changes across the Amazon lowlands over the past 45,000 years. *Nature* 541, 204–207.

Wang, Y.J., et al. 2001 A High-Resolution Absolute-Dated Late Pleistocene Monsoon Record from Hulu Cave, China. *Science*, 294, 2345–2348.

Wigley, T. & M. Brown, 1976: The Physics of Caves. In: T. Ford & C. Cullingford (eds.), *The Science of Speleology*. Academic Press, pp. 329–358, New York, pp. 329–358.

Zomer RJ, Trabucco A, Bossio DA, van Straaten O, Verchot LV, 2008. Climate Change Mitigation: A Spatial Analysis of Global Land Suitability for Clean Development Mechanism Afforestation and Reforestation. *Agric. Ecosystems and Envir.* 126: 67-80.

Zomer RJ, Bossio DA, Trabucco A, Yuanjie L, Gupta DC & Singh VP, 2007. Trees and Water: Smallholder Agroforestry on Irrigated Lands in Northern India. Colombo, Sri Lanka: International Water Management Institute. pp 45. (IWMI Research Report 122).

## **Acknowledgements**

Ideas in this paper were developed thanks to discussions around the NOAA Last Millennium Reanalysis project. We thank Alan Griffiths for providing AWRA-L PET results. Funding is gratefully acknowledged by MOC for an Independent Research Fellowship from the UK Natural Environment Research Council (NE/P017819/1).

## **Author contributions**

Paper conceived by AB and WD, with input from JB, SH and PCT, and analyses by AB and MOC.

Table 1. Global compilation of sites using in this paper. Mean annual temperature and total annual precipitation are from local measurements reported in the publications, with the exception of total annual rainfall at the Borneo sites, where total annual precipitation data was not reported and gridded data is used. Total annual evapotranspiration and the aridity index are sourced from the WorldClim gridded database.

Region	Cave	Lat	Long	Mean Annual Temperature (T)	Total Annual Precipitation (P)	Total Annual Potential Evapotranspiration (PET)	Aridity Index (P/PET)	Weighted Annual Mean $\delta^{18}\text{O}$ Precipitation ( $\delta^{18}\text{O}_p$ )	Annual Mean $\delta^{18}\text{O}$ Drip Water ( $\delta^{18}\text{O}_{dw}$ )	Offset $\Delta(p-dw)$
				(°C)	(mm)	(mm)	(mm)	(‰)	(‰)	(‰)
Australia	Cathedral Cave, NSW (Cuthbert et al., 2014)	32°37'S	148°56'E	18.2	629	1461	0.45	-4.34	-2.81	-1.53
									-2.5	-1.84
									-3.45	-0.89
									-2.43	-1.91
									-1.98	-2.36
									-2.62	-1.72
									-2.9	-1.44
									-2.36	-1.98
									-2.88	-1.46
									-1.96	-2.38
									-2.24	-2.1
									-2.76	-1.58
	-1.51	-2.83								
	-2.19	-2.15								
	-3.30	-1.04								
	Golgotha Cave, WA (Treble et al., 2015)	34.10°S	115.03°E	14.8	1113	1046	1.06	-4.02	-4.00	-0.02
									-3.84	-0.18
									-3.80	-0.22
-4.75									0.73	
-4.02									0.00	
Harrie Wood Cave, NSW (Tadros et al., 2017)	35°43'S	148°29'E	11.1	1177	1098	1.07	-6.85	-6.60	-0.25	
								-6.81	-0.04	
Little Trimmer Cave, TAS (Goede et al., 1983)	41°33'S	146°15'E	9.5	1061	860	1.68	-5.4	-6.76	-0.09	
								-5.04	-0.36	
Frankcombe Cave, TAS (Goede et al., 1983)	42°32'S	146°27'E	8.3	1230	874	1.43	-5.27	-5.04	-0.36	
								-5.26	-0.01	
								-5.38	0.11	
China		24°07'N	104°08'E	16.7	1143	1280	0.76	-10	-9.5	-0.5

	Xianren Cave, Yunnan (Duan et al., 2016)								-9.6	-0.4
									-9.4	-0.6
									-9.3	-0.7
									-9.3	-0.7
	Baojinggong Cave, Guangdong (Duan et al., 2016)	24°07'N	113°21'E	21.2	1836	1325	1.39	-6.9	-5.8	-1.1
									-5.8	-1.1
									-5.1	-1.8
									-5.4	-1.5
									-5.9	-1.1
	Liangfeng Cave, Guizhou (Duan et al., 2016)	26°16'N	108°03'E	18.5	1212	1121	1.12	-7.2	-7.5	0.3
									-6.9	-0.3
									-6.1	-1.1
	Furong Cave, Chongqing (Duan et al., 2016)	29°13'N	107°54'E	17.4	1027	1122	1.07	-6.3	-7.2	0.9
									-7.2	0.9
									-7.2	0.9
									-7.6	1.3
									-7.6	1.3
	Penglaixian Cave, Anhui (Duan et al., 2016)	30°14'N	117°32'E	16.1	1781	1082	1.36	-7.9	-7.5	-0.4
									-7.3	-0.6
									-7.2	-0.7
									-7.3	-0.6
	Heshang Cave, Hubei (Duan et al., 2016)	30°27'N	110°25'E	16.5	1343	1115	1.04	-7.9	-7.2	-0.7
									-7.3	-0.6
									-7.4	-0.5
									-6.9	-1.0
	Wanwang Cave, Gansu (Duan et al., 2016)	33°10'N	105°00'E	14.9	461	1068	0.57	-8.3	-9.1	0.8
									-9.1	0.8
									-9.1	0.8
	Shihua Cave, Beijing (Duan et al., 2016)	39°47'N	115°56'E	12.2	539	992	0.59	-8.7	-8.9	0.2
									-8.8	0.1
									-8.8	0.1
									-8.9	0.2
									-8.9	0.2
Europe	Uamh an Tartair, UK Fuller et al (2008)	58°8'N	4°56'W	7.1	1955	493	2.39	-7.1	-6.90	-0.2
									-7.27	0.17
									-7.18	0.08
									-6.89	-0.21
									-6.92	-0.18
									-7.22	0.12
									-7.21	0.11
									-7.13	0.03
									-6.97	-0.13
									-7.00	-0.1
									-7.07	-0.03
									-7.07	-0.03

									-7.30	0.20
	Grotte de Villars, France (Genty et al., 2014)	45°26'N	0°47'E	12.4	1005	963	0.96	-6.2	-6.38	0.18
									-6.39	0.19
									-6.17	-0.03
									-6.17	-0.03
	Chauvet Cave, France (Genty et al., 2014)	44°23'N	4°24'E	14.1	779	983	0.79	-6.6	-6.89	0.29
North America	West Cave, TX (Feng et al., 2014)	30°20'N	98°8'W	20	813	1484	0.55	-4.1	-4.43	0.33
									-4.41	0.31
									-4.41	0.31
	Inner Space, TX (Pape et al., 2010)	30°36'N	97°41'W	19.2	848	1453	0.58	-4.1	-4.4	0.3
									-4.4	0.3
	Caverns of Sonora, TX (Pape et al., 2010)	30°33'N	100°49'W	17.9	536	1574	0.34	-4.1	-5.17	1.07
									-4.97	0.87
									-4.71	0.61
	Natural Bridge Cave, TX (Pape et al., 2010)	29°41'N	98°20'W	19.6	740	1478	0.55	-4.1	-4.33	0.23
									-4.55	0.45
									-4.17	0.07
									-4.16	0.06
								-4.31	0.21	
Borneo	Lang's Cave and Wind Cave (Partin et al., 2013; Moerman et al., 2014)	4'02	114'48	25	3842	1472	2.61	-8.6	-8.4	-0.2
									-8.2	-0.4
									-8.0	-0.6

Figure 1. Location of the cave sites in comparison with (a) mean annual temperature, (b) aridity index (P/PET).

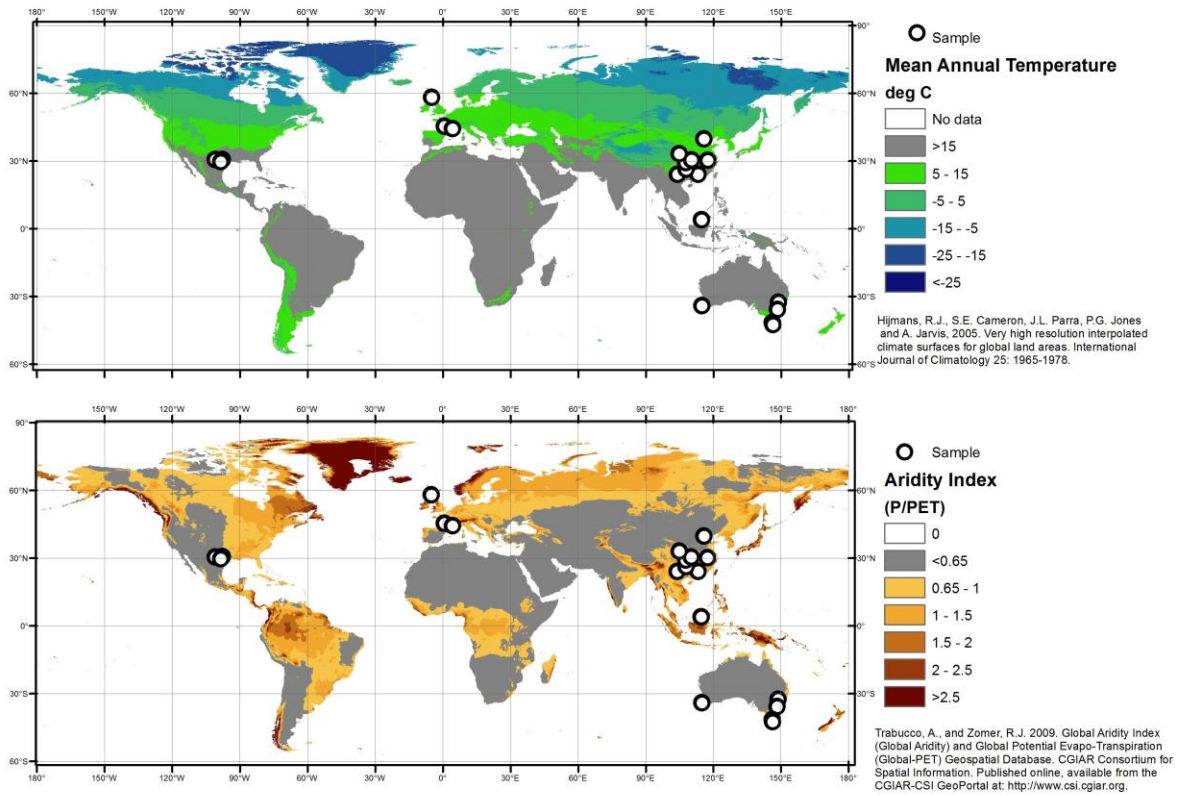


Figure 2. Correlation matrices for the climate and cave drip water parameters. The frequency distribution for each parameter is shown along the cross-axis. Where the relationship between parameters is statistically significant, the regression line and  $R^2$  value is shown. 95% confidence ellipses are presented for all correlation matrices. For abbreviations see Table 1.

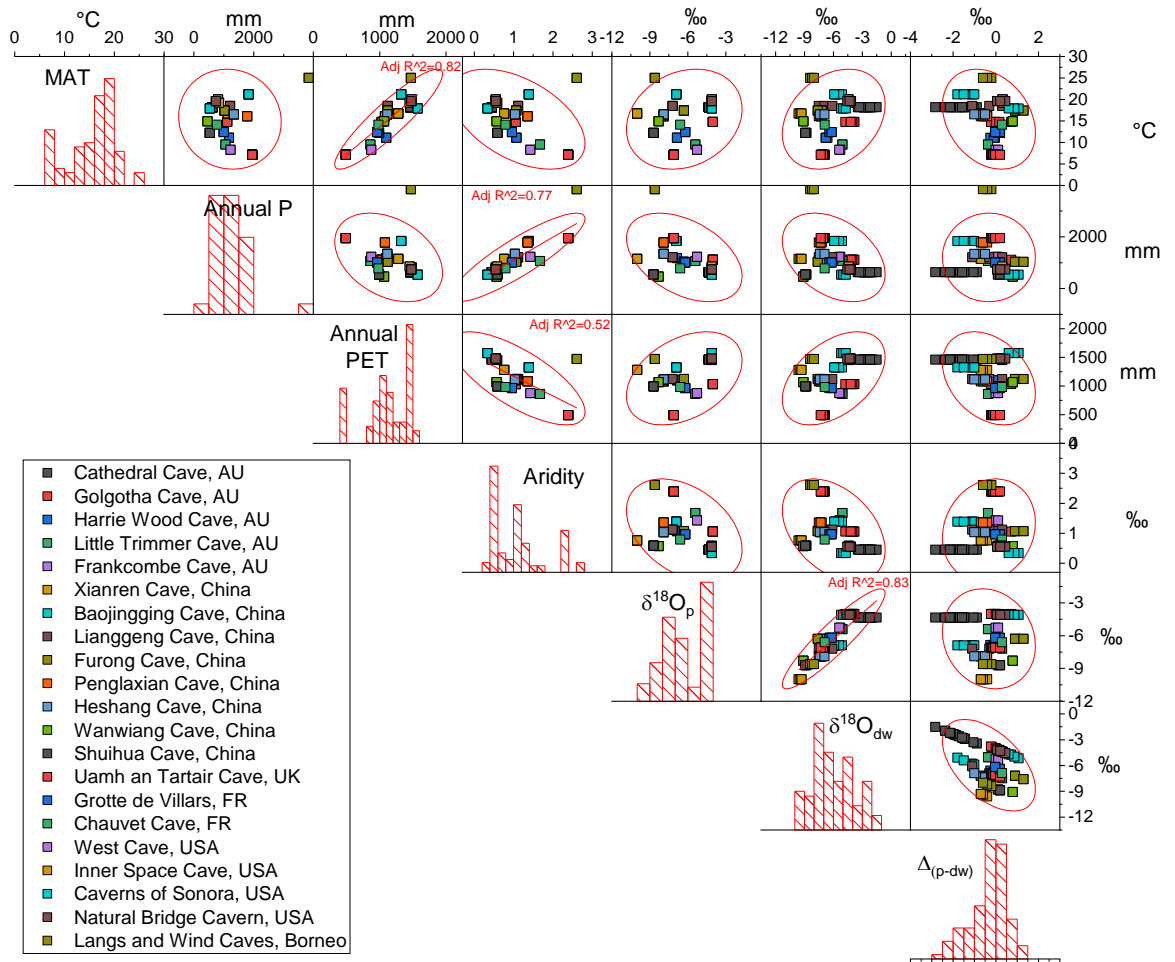
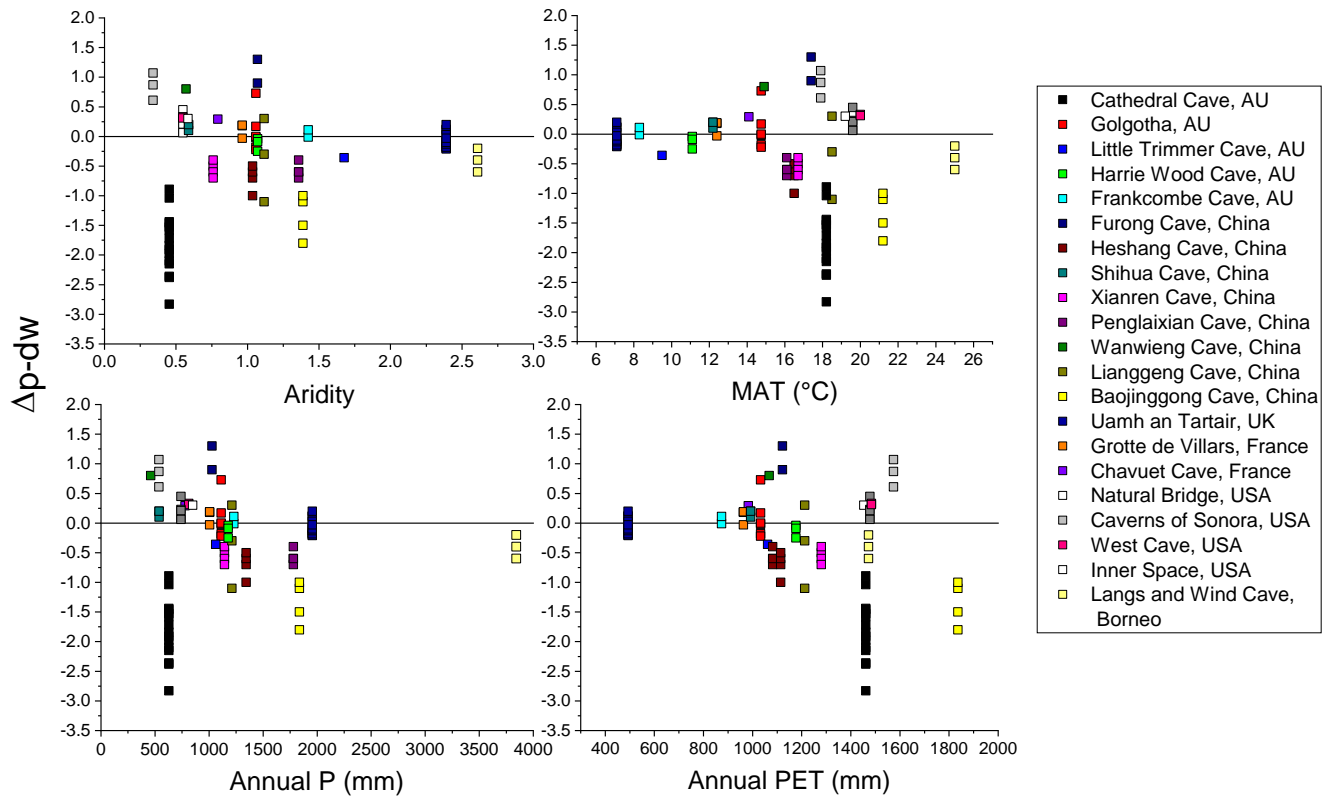


Figure 3. Scatter plots of the relationship between four climate parameters and the difference between precipitation and drip water  $\delta^{18}\text{O}$  (a) aridity index (b) mean annual temperature (c) total annual precipitation and (d) total annual PET.



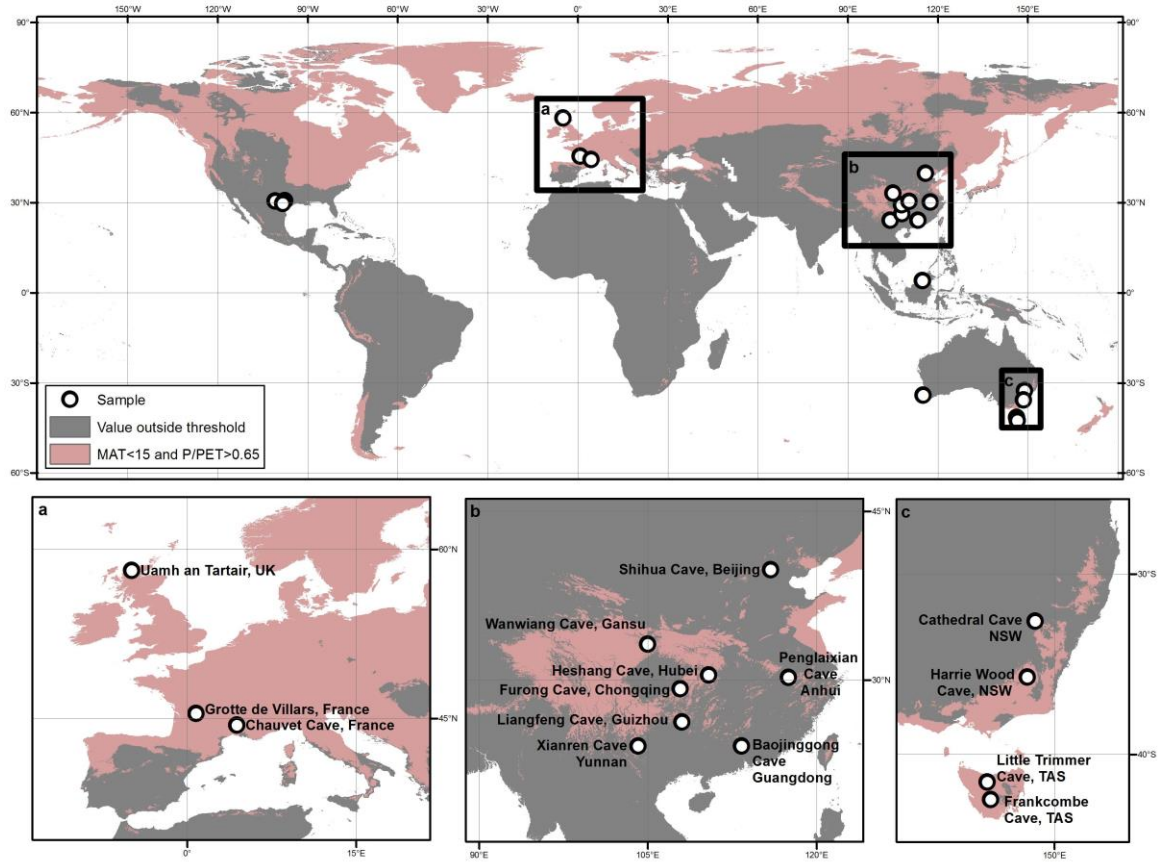


Figure 4. Location of the cave sites in comparison with the thresholds of MAT < 15 °C and P/PET > 0.65. (a) Europe (b) Chinese monsoon region and (c) SE Australia.